



14th Deep Sea Offshore Wind R&D Conference, EERA DeepWind'2017, 18-20 January 2017, Trondheim, Norway

## A 3D FEM model for floating wind turbines support structures

Campos A<sup>a</sup>, Molins C<sup>a\*</sup>, Trubat P<sup>a</sup>, Alarcón D<sup>a</sup>

<sup>a</sup> *Universitat Politècnica de Catalunya, C/Jordi Girona 1-3 CN C1-206. Barcelona, 08034, Spain*

---

### Abstract

The relevance of the interaction between the structural stiffness and the wind turbine dynamics are well known by the industry from decades of expertise. However, the novel floating concepts are commonly designed by tools that disregard the individual structural stiffness of the elements which compose the floating platform. Usually, these elements are treated as rigid body elements in the design process. However, their flexibility can be relevant in the long time structural life assessment, particularly for the fatigue assessment. Then, a structural analysis that includes the dynamic effects over the deformation of the structure is required. The paper proposes a model that integrates the instantaneous deformation of the structure by a nonlinear dynamic Finite Element Analysis (FEA) computation in a fully coupled Offshore Wind Turbine (WT) model in the time domain.

A 3D hydro-aero-servo-elastic coupled numerical model in time domain for structural analysis of floating or bottom fixed structures has been developed at the UPC-BarcelonaTech. The code integrates the forces exerted by the waves and currents as well as the aerodynamic loads, including the wind turbine, and the mooring system. For the hydrodynamic loads the Morison's equation is used to compute waves and current forces. Both Airy (regular and irregular) and Stokes 5th order wave theories are implemented. The mooring system can be computed in a quasi-static way or considering their fully dynamics. The aerodynamic loads are computed with AeroDyn standalone module from NREL, which is coupled to the FE model. The structure is discretized with one-dimensional beam finite elements, in which the formulation considers small strains as well as large motions under the implementations of the Euler beams theory. With this approach, the dynamic interaction between the wind turbine and the structure, as well as the effects on the internal forces are implicitly coupled in the formulation.

A comparison of the Windcrete concrete SPAR concept experimental Response Amplitude Operators (RAO) against the numerical results are presented, as well as some results from simulations under normal operation conditions.

© 2017 The Authors. Published by Elsevier Ltd.  
Peer-review under responsibility of SINTEF Energi AS.

*Keywords:* Wind; Energy; Structures; Wind turbines; Offshore; Dynamic analysis; Floating; Renewables

---

\* Corresponding author. Tel.: +34 93 401 10 53.  
E-mail address: [climent.molins@upc.edu](mailto:climent.molins@upc.edu)

## 1. Introduction

The dynamic analysis of floating offshore platforms has been typically done by assuming the rigid body approach for those structures. That approach is commonly accepted for most offshore structures, in which their dimensions and proportions are large enough to neglect the second order effects produced by the deformation of the structure.

Consistently, the most commonly used commercial software compute the overall motions of the floating structures assuming the floating substructures as rigid bodies [1], [2]. Additionally, they do not take into account the instant position for load calculations as shown in [3]. Then, the computed loads and accelerations are integrated in a linear or nonlinear static Finite Element Analysis (FEA) [2]. This methodology permits to consider the effects of the structural deformations for the internal forces computation, but it does not consider the effects of those deformations in the computation of the overall motions of the floating system, which can lead to different internal forces, as well as modify the wind turbine – structure interaction. Also the effects of the dynamic interaction between the fluid and the substructure deformations have to be analyzed, as can be deduced from the work of Borg et.al. [4].

To deal with that matter, the paper presents a coupled hydro-aero-servo-elastic dynamic 3D FE numerical model capable to analyze floating support structures for offshore wind turbines (WT) developed at the UPC-BarcelonaTech. The model has been named as FloaWDyn can also analyze bottom fixed offshore and onshore WT support structures, including the whole structural flexibility, from the floater up to the WT.

The paper presents a brief description of the theoretical basis of the model, followed by the Response Amplitude Operators (RAO's) comparison between the experimental results obtained during the Windcrete experimental campaign, performed at the UPC-BarcelonaTech wave flume, and the simulations performed with FloaWDyn, in which the model is adjusted from the experimental collected data. Also some results from a simulation of the Windcrete concept, supporting the NREL 5MW wind turbine, under normal operational wind and waves conditions are presented.

## 2. The numerical model

A 3D nonlinear coupled aero-hydro-servo-elastic dynamic finite element numerical model has been developed to analyze the structural behavior of WT supporting structures, both onshore and offshore, in the time domain. The model assumes small strains but considers large displacements. First, the basics of the FE model formulation are presented including the co-rotational approach to deal with large body motions. Second, the key aspects of the dynamic formulation are described including the integration scheme. Then, basic details of the procedures for accounting for the hydrodynamic, the aerodynamic and the mooring system loads are described.

### 2.1. FEM discretization

The FE numerical model is based in the Euler beam theory, which in combination with elasticity and one-dimensional finite elements may be used to analyze the most common types of onshore and offshore wind turbines support structures.

The relationship between the nodal displacements and the internal forces is derived by applying the virtual work principle [5]. From the Euler beam theory, the following relations between the element transversal ( $w$ ) and axial ( $u$ ) displacements and the resulting strain ( $\varepsilon$ ) can be expressed as shown in eq. (1), while the strains from the torsional effects ( $\varepsilon^T$ ) can be expressed as shown in eq. (2).

$$\varepsilon = \frac{\partial u}{\partial x} + z_l \chi \quad ; \quad \chi = \frac{\partial^2 w}{\partial x^2} \quad (1)$$

$$\varepsilon^T = r \frac{\partial \theta}{\partial x} \quad (2)$$

where:

$z_l$  and  $r$  are the distances from the neutral axis to the farthest point from this axis in the analysed cross section.

$\chi$  is the curvature of the cross section.  
 $\theta$  is the torsional angular distortion.

The resulting stiffness matrix for each element can be expressed as eq. (3), where  $\mathbf{D}$  is the constitutive material matrix from the elasticity [6], and  $\mathbf{B}$  is the corresponding derivatives of the shape functions [5].

$$\mathbf{K}^e = \iiint_{V^e} \mathbf{B}^{eT} \cdot \mathbf{D} \cdot \mathbf{B}^e \cdot dV \tag{3}$$

Finally, the system of equations to solve can be expressed as (4), where  $\mathbf{f}^e$  are the local forces applied to the element and  $\mathbf{x}^e$  are the nodal displacements of the element in its local coordinates, having 12 degrees of freedom (DOF) per element.

$$\mathbf{f}^e = \mathbf{K}^e \cdot \mathbf{x}^e \tag{4}$$

The numerical model is capable to deal with multiple materials on a same structure, including the addition of rigid links. Those elements acts as rigid bars, without contributing to the self-weight neither to the external loads.

Rigid elements are useful to increase the fidelity of the simulation when different FE converges into the same node and they have very different sectional dimensions. The “gap” between the discretized beam end point and its adjacent beam centreline is connected by the rigid links. The same approach can be used to simulate the mooring system connection to the structure (fairleads) for floating structures.

### 2.2. Co-rotational approach

In order to be able to analyze floating structures with large rigid body motions but small strains, a consistent co-rotational formulation for dynamic analysis proposed by Crisfield [7] is implemented. This formulation allows the computation of the equivalent local angles with respect a co-rotational frame, which is moving attached to the element as shown in Figure 1. As can be observed in Figure 1, the nodal triads  $T'$  and  $U'$  rotate rigidly attached to the element nodes, while triad  $E'$  is computed from the combination of triads  $T'$  and  $U'$  and the imaginary line connecting the element nodes.

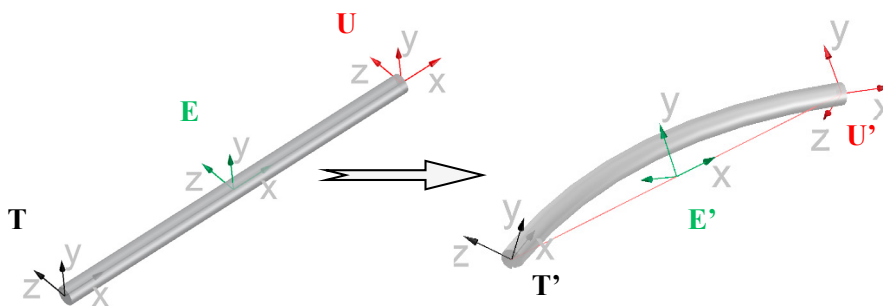


Figure 1: 3D Co-rotational frame. Undeformed (left) and deformed element (right)

Computing the relative angle between the triads  $T'$  and  $U'$  against triad  $E'$  [8], the nodal displacements can be split into rigid body motions and internal deformations  $\mathbf{d}_e$ . Once the internal deformations are computed, combining it with the stiffness properties shown in section 2.1, the internal forces can be finally computed.

### 2.3. Dynamic analysis

The equations of motion of the global system are obtained by the application of the Newton’s second law, equation (5). Thus, d’Alembert’s principle is applied, from which the external, internal and inertial forces should be at equilibrium at each time step. To integrate the 2<sup>nd</sup> order effects related to the large displacements the geometry of the structure is updated at each iteration, as well as the internal forces  $\mathbf{F}_{int}^{e^t}$ . The solution of the system of equations yields to the increment of displacements between time steps in global coordinates. Matrix  $\mathbf{T}_e$  is the standard rotation matrix at each iteration used to update to the new geometry based on the initial configuration.  $\mathbf{M}_e$  is the local diagonal mass matrix, including the rotational moment of inertia of the element and the added mass terms in the case of floating platforms.

$$\underbrace{\left(\mathbf{T}_e^{Tt} \cdot \mathbf{M}_e^t \cdot \mathbf{T}_e^t\right)}_m \cdot \delta \ddot{\mathbf{X}}_e^{t+\Delta t} + \underbrace{\left(\mathbf{T}_e^{Tt} \cdot \mathbf{C}_e^t \cdot \mathbf{T}_e^t\right)}_c \cdot \delta \dot{\mathbf{d}}_e^{t+\Delta t} + \underbrace{\left(\mathbf{T}_e^{Tt} \cdot \mathbf{K}_e^t \cdot \mathbf{T}_e^t\right)}_k \cdot \delta \mathbf{X}_e^{t+\Delta t} = \mathbf{F}_{ext}^{e^t} - \mathbf{F}_{int}^{e^t} \quad (5)$$

Since vector  $\mathbf{X}_e$  refers to global displacements, including rigid body motions, the structural damping matrix  $\mathbf{C}_e$  should only affect to the equivalent local displacements velocity vector  $\dot{\mathbf{d}}_e$ . Rayleigh damping is assumed, so the  $\mathbf{C}_e$  matrix is computed as a linear combination of the mass and the stiffness matrices [9].

For the time integration of the equations of motion, the Hilber-Hughes-Taylor (HHT) scheme [10] is adopted. Setting the value of the amount of artificial damping  $\alpha$  and its associated  $\gamma$  and  $\beta$  Newmark’s values, an incremental relationship of the form of  $\Delta \mathbf{F} = \mathbf{K} \cdot \Delta \mathbf{X}$  can be expressed as (6), where  $\mathbf{Q}_a$  is a vector related to the HHT time integration scheme,  $\Delta t$  is the time step and  $\mathbf{F}_{D,int}$  is the vector of internal damping forces.

$$\underbrace{\left(\frac{1}{\beta \Delta t^2} \mathbf{M}^t + (1 + \alpha) \mathbf{K}^t\right)}_{\mathbf{K}_{eq}^n} \cdot \Delta \mathbf{X}^{t+1} = \underbrace{(1 + \alpha) \left(\mathbf{F}_{ext}^{t+1} - \left(\mathbf{F}_{int}^t + \mathbf{F}_{D,int}^t\right)\right) - \alpha \left(\mathbf{F}_{ext}^t - \left(\mathbf{F}_{int}^t + \mathbf{F}_{D,int}^t\right)\right) + \mathbf{M}^t \cdot \mathbf{Q}_a^t}_{\Delta \mathbf{F}} \quad (6)$$

### 2.4. Hydrodynamic loads

For the computation of the waves and currents hydrodynamic loads, the Morison’s equation [11] is employed in the model. For its implementation, the following set of hydrodynamic coefficients have to be defined for each element:

- $C_{m,T}$  Transversal inertial coefficient
- $C_{m,L}$  Longitudinal inertial coefficient
- $C_{d,T,q}$  Transversal quadratic drag coefficient
- $C_{d,L,q}$  Longitudinal quadratic drag coefficient
- $C_{d,T,l}$  Transversal linear drag coefficient
- $C_{d,L,l}$  Longitudinal linear drag coefficient
- $C_{a,T}$  Transversal added mass coefficient
- $C_{a,L}$  Longitudinal added mass coefficient

Both  $C_m$  and  $C_d$  coefficients are directly related to Morison’s equation, while  $C_a$  is related to the added mass of the elements. In the case of  $C_d$ , both linear (l subscript) and quadratic (q subscript) coefficients are implemented to adjust the drag forces from experimental data.

As is well known, the application of the Morison's equation requires an estimation of the water kinematics. Currently, Airy (regular and irregular) as well as Stokes 5<sup>th</sup> order waves theories are implemented in the numerical model. In the case of irregular waves, both a user defined spectrum or a wave record data can be used to simulate the water kinematics of the corresponding sea state. In addition, Wheeler's stretching [12] has been implemented to approximate the water kinematics above the mean sea level (MSL) when Airy wave theory is assumed.

The computation of the buoyancy forces is based on the integration of the surface pressures, both hydrostatic and hydrodynamic. To perform the numerical integration of the pressures, a 3D mesh of the external face of the structure is used to obtain at each time step the global position of the mesh elements centroids. Knowing the depth of any point of the mesh, the pressure at the corresponding mesh element can be directly computed. Then, to apply the forces to the FE model, the forces at each 3D element should be collapsed to the structure elements by the sum of the 3D buoyancy forces components from the mesh integration [13].

### 2.5. Aerodynamic loads

Since the numerical model is specifically designed for wind turbine support structures, the aerodynamic loads are separated into two categories: wind loads over the structure and wind loads from the wind turbine (WT). The effect of the wind loads over the structure is implemented in a very similar way as the water viscous loads, but with the corresponding air density and drag coefficients. The relative velocity between the structure and the air,  $\mathbf{v}_r$ , is used to compute the forces acting over the structure (7), where the wind vertical profile is defined as a user input.

$$\mathbf{f}_{D,WIND} = \frac{1}{2} \rho_{air} \cdot A \cdot C_{d,WIND} |\mathbf{v}_r| \mathbf{v}_r \quad (7)$$

The aerodynamic wind turbine loads are computed with the standalone version of the AeroDyn BEM module from NREL [14]. Then, the definition of a user strategy of control for blade collective pitch allows the numerical model to compute the dynamics of the WT by the application of the Newton's 2<sup>nd</sup> law over the applied torque against the residual one from the generator shaft. Since the WT is fully coupled with the structure, the inflow wind depends on the global structure velocities at the hub.

### 2.6. Mooring system loads

For the mooring system, the numerical model includes two different methods: quasi-static moorings and dynamic moorings. For the mooring dynamics, a FEM model based on the formulation presented by Garret [15], with the addition of material stiffness and small strains assumption based on the work of Kim [16] is employed.

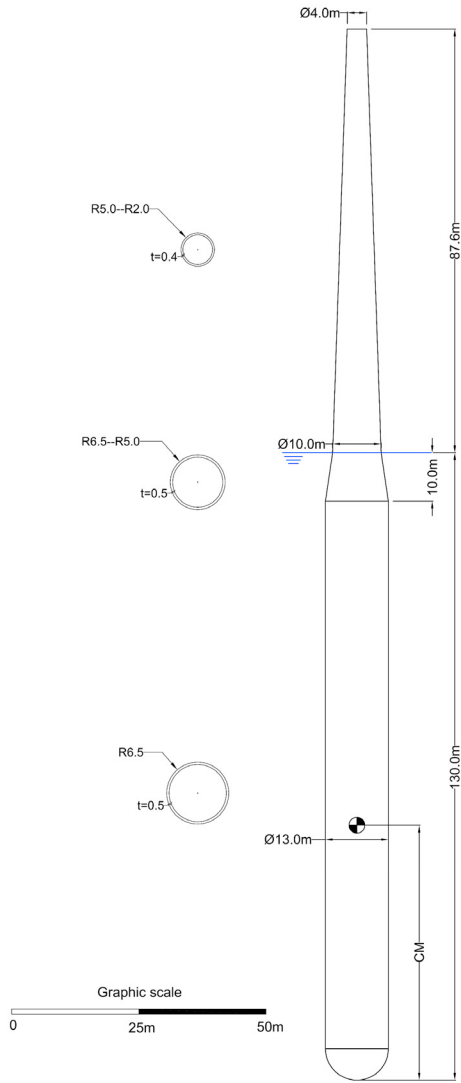
### 2.7. Other loads

The numerical model includes the possibility to add any kind of load applied to the structure a part from the hydro and aerodynamic loads. Those loads include the structure self-weight, user defined lumped masses, the possibility to add ballast weight into the desired elements for floating structures and other user defined forces applied on the structure nodes.

## 3. Numerical tests validation

For the validation of the presented numerical model, a set of different structures under multiple load cases are modelled for comparison. In the following section, some simulations of the Windcrete [17] simulations are presented. The Windcrete concept is a monolithic concrete SPAR type floating concept for WT's (Figure 2). A set of regular and irregular waves load cases as well as free decay tests were applied to the scaled model to obtain, amongst other data, the experimental RAO's [18] and the hydrodynamic coefficients in the frame of the KIC-InnoEnergy AFOSP

innovation project [19]. Drag, inertial and added mass coefficients in the numerical model are adjusted based on the experimental free decay and regular wave tests. The most relevant parameters of the Windcrete concept are summarized in Table 1.



Property	Value
Displaced Volume [m <sup>3</sup> ]	1.69E+4
Draft [m]	130.0
Concrete mass [kg]	8.71E+6
Ballast mass [kg]	8.34E+6
Wind turbine mass [kg]	3,50E+5
CM [m]	53.34
CB [m]	63.97
Metacentric height [m]	10.57
Floater C <sub>dT,q</sub>	0.7
Floater C <sub>dL,q</sub>	1.3
Floater C <sub>mT</sub>	1.8

Table 1: Windcrete main properties

Figure 2: Windcrete SPAR concept

The Response Amplitude Operators (RAO) comparison between the experimental and the numerical results is shown in **Error! No s'ha trobat l'origen de la referència..** As can be observed, both pitch and heave eigenperiods are well captured, being 30s the heave eigenperiod and 40s the pitch/roll eigenperiod. Also the magnitude of the RAO for all the analysed frequencies are consistent between the simulations and the experimental results.

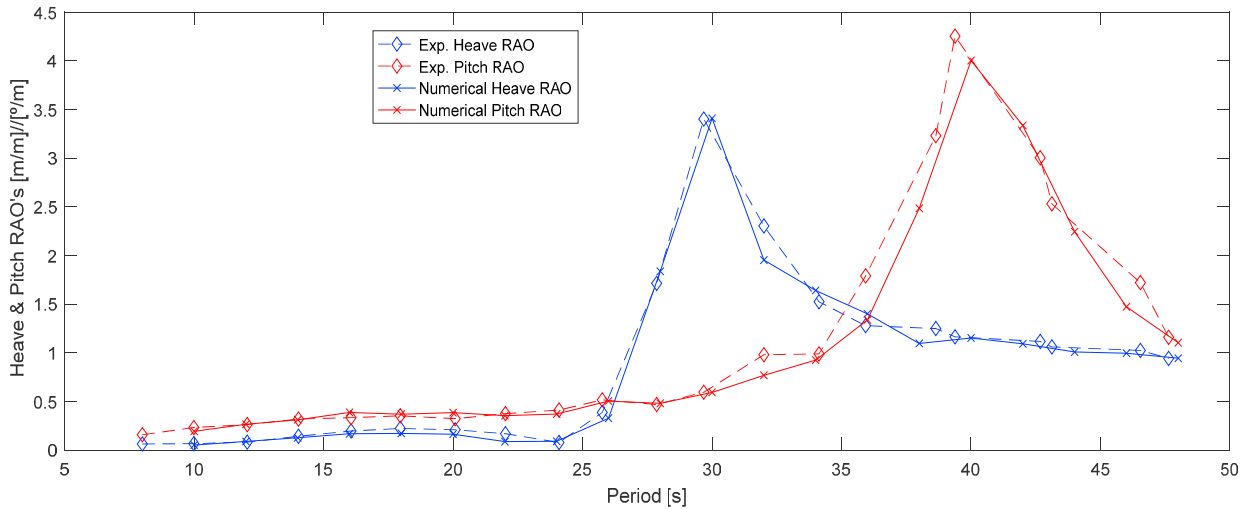


Figure 3: Experimental vs numerical RAO's comparison

With the numerical model properly adjusted to the experimental results, some relevant results from a normal operational conditions simulation are presented. The simulation includes the effect of the NREL 5MW [20] wind turbine under a mean wind value of 12m/s and Normal Turbulence Model (NTM) model, including the control strategy defined by Jonkman *et.al* [20]. The sea state is computed as irregular Airy waves based on a JONSWAP spectrum with  $H_s=7.1\text{m}$ ,  $T_p=12.1\text{s}$  and  $\gamma=72.2$ .

The simulation results are shown in Figure 4. The figure shows the time histories of the incident waves and wind as well as the main platform motions (Surge, Heave and Pitch), the top and bottom tower pitch bending moments (PT1 and PT2 respectively) and the nacelle fore-aft acceleration (TTAccFA). Wave and WindVx refers to the wave height and the relative inflow wind at hub height, respectively. As prescribed criteria in the Windcrete predesign [17], under normal operational conditions the maximum pitch inclination is around  $5^\circ$  while the maximum heave motions are consistent with the incident waves and the experimental RAO's. From the point of view of the WT, the nacelle acceleration does not exceed from 0.2g which should be one of the WT's manufacturers requirement. Also in Figure 4 are depicted the bending moments at two different sections of the structure, one placed at the tower base (PT1) and the other placed at 80m from the bottom of the platform (PT2), where the bending moment presents its maximum magnitude in the floater substructure.

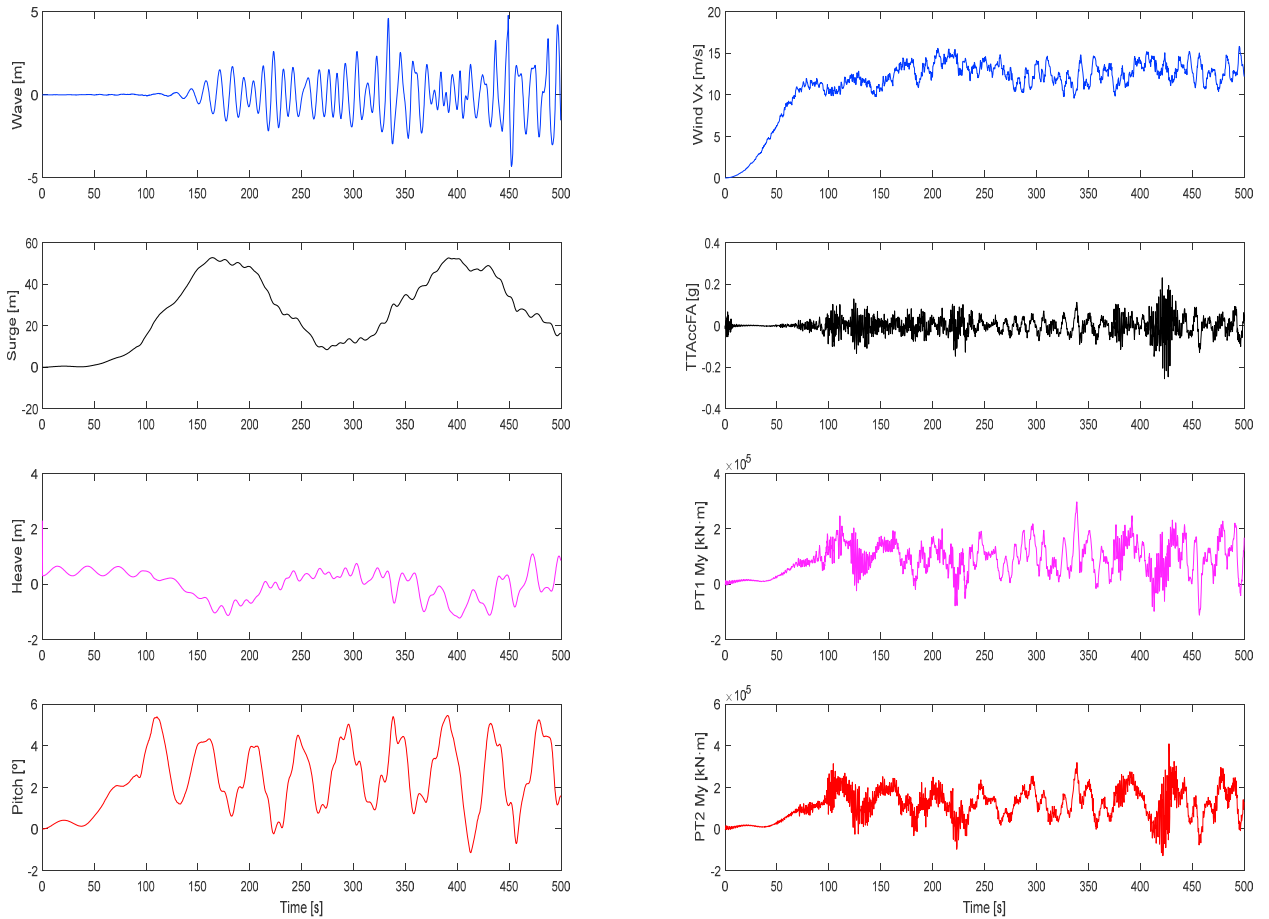


Figure 4: Windcrete normal operational conditions simulation

#### 4. Conclusions

The FloaWDyn numerical model has been proved as a potential powerful tool for the analysis of floating offshore structures, being capable to not only predict the overall motions and dynamics of the structure but also for the time analysis of the internal forces in the floating substructure. The RAO's validation shows a good agreement between the experimental results with the properly adjusted model in the numerical simulations. Both the magnitude and the frequency are well captured. For the numerical simulation under normal operation conditions, the predesign expectations regarding the maximum inclinations and nacelle accelerations are matched, being under  $5^\circ$  and  $0.2g$  correspondingly.

The numerical tool is very interesting for research purposes because permits an easy addition of new modules with new features and multitude of parameters to adjust the models. At the present time, a 3D shell FEM module in combination with the current beam elements module is under development, increasing the scope of the structural typologies which would be possible to simulate with high accuracy. This new implementation will include the possibility of the use of potential flow theory, importing the hydrodynamic results from specialized and well known commercial software as NEMOH [21], WAMIT [22] or AQWA [2].

## Acknowledgements

The experimental results presented this paper were obtained during the KIC Innoenergy (EIT) AFOSP innovation project (Alternative Floating Offshore Support Platform), which financial support is greatly appreciated. We would also like to express our gratitude to the Catalan government for the financial support through its AGAUR agency.

## References

- [1] B. Jonkman and J. Jonkman, “FAST v8.16.00a-bjj,” 2016.
- [2] ANSYS, “AQWA User’s manual.” 2012.
- [3] R. Antonutti, C. Peyrard, L. Johanning, A. Incecik, and D. Ingram, “The effects of wind-induced inclination on the dynamics of semi-submersible floating wind turbines in the time domain,” *Renew. Energy*, vol. 88, pp. 83–94, 2016.
- [4] M. Borg, A. M. Hansen, and H. Bredmose, “Floating substructure flexibility of large-volume 10MW offshore wind turbine platforms in dynamic calculations,” *J. Phys. Conf. Ser.*, vol. 82024, 2016.
- [5] O. C. Zienkiewicz, *The finite element method*, 6th ed. 2006.
- [6] S. Rao, *The finite element method in engineering*, 2nd ed. Pergamon Press, 1989.
- [7] M. A. Crisfield, *Nonlinear Finite Element Analysis of Solids and Structures*, vol. 2. John Wiley & Sons Inc, 1997.
- [8] R. A. Spurrier, “Comment on ‘singularity-free extraction of a quaternion from direction cosine matrix,’” *J. Spacecr.*, no. 15, p. 255, 1978.
- [9] A. Alipour and F. Zareian, “Study Rayleigh Damping in Structures; Uncertainties and Treatments,” in *14 th World Conference on Earthquake Engineering: Innovation Practice Safety*, 2008.
- [10] H. M. Hilber, T. J. R. Hughes, and R. L. Taylor, “Improved numerical dissipation for time integration algorithms in structural dynamics,” *Earthq. Eng. Struct. Dyn.*, no. 5, pp. 283–292, 1977.
- [11] J. Morison, “The force distribution exerted by surface waves on piles,” 1953.
- [12] J. Wheeler, “Methods for Calculating Forces Produced by Irregular Waves,” *J. Pet. Technol.*, vol. 22, no. 3, 1970.
- [13] A. Campos, M. Molins, P. Trubat, and D. Alarcón, “Analysis of Structural Second Order Effects on a Floating Concrete Platform for FOWT’s,” *Energy Procedia*, vol. 94, no. January, pp. 155–163, 2016.
- [14] P. J. Moriarty and a C. Hansen, “AeroDyn Theory Manual,” Golden, 2005.
- [15] D. L. Garrett, “Dynamic Analysis of Slender Rods,” *J. Energy Resour. Technol.*, vol. 104, no. 4, pp. 302–306, 1982.
- [16] Y.-B. Kim, “Dynamic Analysis of multiple-body floating platforms coupled with mooring lines and risers,” Texas A&M University, 2003.
- [17] A. Campos, C. Molins, X. Gironella, and P. Trubat, “Spar concrete monolithic design for offshore wind turbines,” *Proc. Inst. Civ. Eng. - Marit. Eng.*, vol. 169, no. 2, pp. 49–63, Jun. 2016.
- [18] A. Campos, C. Molins, X. Gironella, P. Trubat, and D. Alarcón, “Experimental rao’s analysis of a monolithic concrete spar structure for offshore floating wind turbines,” in *Proceedings of the 34th International Conference on Ocean, Offshore and Arctic Engineering. OMAE 2015*, 2015, pp. 1–9.
- [19] C. Molins, A. Campos, P. Trubat, D. Alarcon, X. Gironella, and P. Roca, “KIC-InnoEnergy AFOSP – WP4 : SCALED TESTING,” 2014.
- [20] J. Jonkman, S. Butterfield, W. Musial, and G. Scott, “Definition of a 5-MW reference wind turbine for offshore system development,” *Contract*, no. February, pp. 1–75, 2009.
- [21] LHEEA, “NEMOH User’s manual.” École Central de Nantes, Nantes (France), 2014.
- [22] C. H. Lee and J. N. Newman, “WAMIT User manual.” WAMIT Inc, 2006.